Optical Characterization of Heat Transport in Vertically Aligned Carbon Nanotube Arrays

by

Sara Margala

A Thesis Submitted to the Faculty of the

JAMES C. WYANT COLLEGE OF OPTICAL SCIENCES

In Partial Fulfillment of the Requirements

For the Degree of

MASTER OF SCIENCE

In the Graduate College

THE UNIVERSITY OF ARIZONA

2024

THE UNIVERSITY OF ARIZONA
GRADUATE COLLEGE

As members of the Master's Committee, we certify that we have read the thesis prepared by **Sara Grace Margala**, titled ***Optical Characterization of Heat Transport in Vertically Aligned Carbon Nanotube Arrays,*** and recommend that it be accepted as fulfilling the dissertation requirement for the Master's Degree.

_________________________ Date: 24 JUL 2024
Professor Ronald G. Driggers

_________________________ Date: 7/24/2024
Professor Daewook Kim

_________________________ Date: 8/6/24
Dr. David W. Young

Final approval and acceptance of this thesis is contingent upon the candidate's submission of the final copies of the thesis to the Graduate College.

I hereby certify that I have read this thesis prepared under my direction and recommend that it be accepted as fulfilling the Master's requirement.

_________________________ Date: 24 JUL 2024
Professor Ronald G. Driggers
Master's Thesis Committee Chair
Wyant College of Optical Sciences

TABLE OF CONTENTS

LIST OF FIGURES

ABSTRACT

Vertically aligned carbon nanotube (VACNT) arrays, absorbing virtually all incident light, are a novel material with unique applications including as sensors, solar energy converters, and as nearly ideal blackbody radiators. Their superior thermal and optical properties are attributed to their structure, which can vary with how they are grown. In applications where insulation between tubes is of high importance, measurement of transverse thermal diffusivity is critical. In contrast with methods that measure transverse thermal diffusivity by measuring the back surface, here, the distal ends of the nanotubes are flash-irradiated with a Gaussian laser pulse with 1 µm wavelength and the infrared emission of the VACNT front surface is captured as a function of time. Analysis of the captured images provides measurement of the thermal diffusivity in the transverse direction of the VACNT array. This method has been used for other anisotropic materials, but has not yet been applied to VACNT arrays. The optical characterization method demonstrated here enables feedback for application-tailored optimization of VACNT synthesis processes.

Chapter 1: Introduction

Carbon can exist in many different forms such as coal, diamond, graphene, amorphous carbon, and fullerenes. A hollow cylinder of graphene forms another allotrope—a carbon nanotube (CNT). CNTs are described as either Single-Walled (SWCNTs) or Multi-Walled (MWCNTs), referring to how many concentric layers of graphene make up a singular tube. Illustrations of these different forms are shown in Figure 1. If many SWCNTs or MWCNTs are assembled parallel to each other in a direction normal to their substrate, they are considered vertically aligned carbon nanotubes (VACNTs). A scanning electron microscope (SEM) image of VACNTs viewed from the side is show in Figure 2. Diameters of individual tubes are on the scale of nanometers. The lengths of tubes range from microns to multiple millimeters. The thermal and optical properties of VACNTs make them highly desirable for many applications. CNTs are extremely good thermal conductors along the tube axis, and good thermal insulators perpendicular to the tube axis. Thermal conductivity for individual MWCNTs have been reported up to 3000 W/m*K along the tube axis [1]. Perpendicular to the tube axis, thermal conductivities around 1.5 W/m*K have been reported [2]. CNTs are also one of the most absorptive materials known to exist [3]. Because of these unique properties, VACNT arrays have a wide range of applications spanning many fields including optical, mechanical, and electrical engineering. Some specific applications include heat management systems, stray light mitigation, pyroelectric sensors, and nearly ideal blackbody radiators [4] [5] [6].

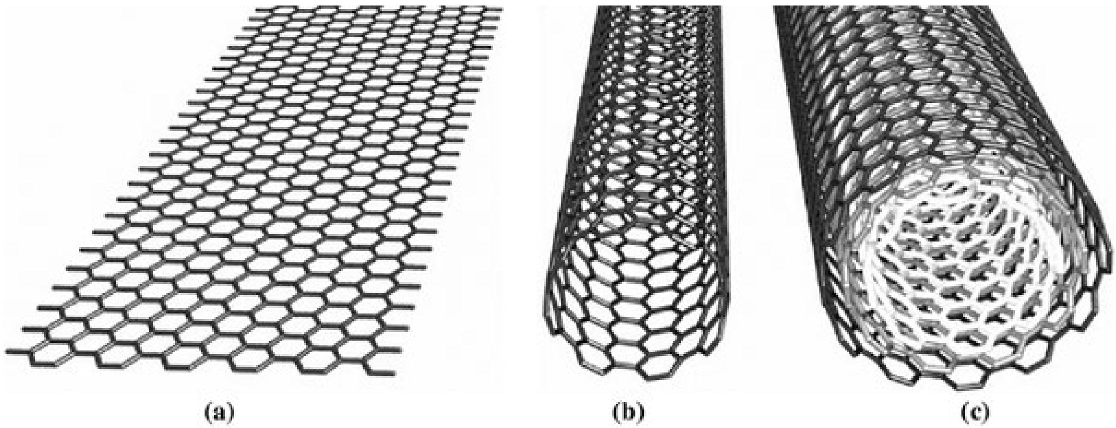

Figure 1. a. Graphene sheet, b. singular SWCNT, c. singular MWCNT [7].

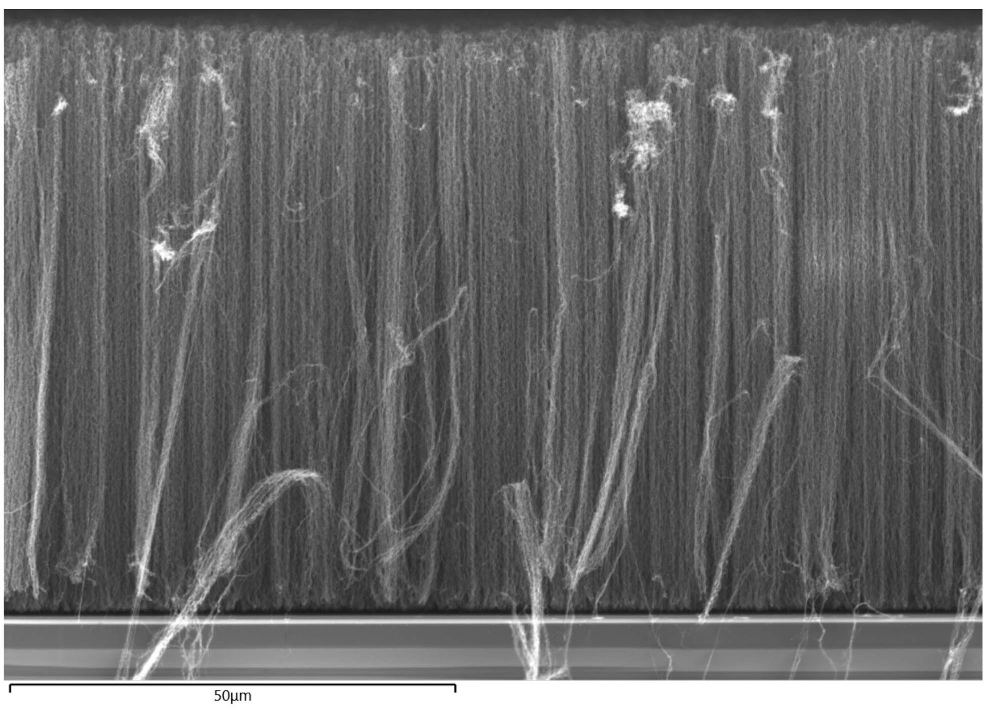

Figure 2. Scanning Electron Microscope (SEM) image of VACNTs. SEM used is FEI Scios™ dual beam.

Chapter 2: Background

Section 2.1 Synthesis of Vertically Aligned Carbon Nanotubes

VACNTs can be grown by different techniques such as electrical discharge in the presence of a gaseous hydrocarbon, or through the use of chemical reactions using a catalyst. The latter process, referred to as chemical vapor deposition, or CVD, is what was used to create the multi-walled VACNTs measured in this work. An overview of this process is shown in Figure 3. There are many different parameters that can be varied for each step of the VACNT synthesis process. While VACNTs can be grown on a range of materials, silicon wafers are a good option due to their flatness and affordability. The first step in the synthesis process is deposition of a buffer layer on the substrate surface. The purpose of this step is to increase the adhesion of a catalyst to the bare silicon. The buffer layer is deposited onto the surface via an electron beam (e-beam) in a 250 nm thick layer. Next, a thin layer of a metal catalyst, in this case iron, is deposited onto the surface. The metal can be deposited via an electron beam or by sputtering. The synthesis process is very sensitive to the thickness of the catalyst layer. If too little or too much is deposited, CNT growth may be unsuccessful. For successful synthesis of CNTs, the layer thickness of the catalyst must be about 2 nm. The metal catalyst layer naturally forms as small particle “islands” on the surface out of which the CNTs will grow. The particle size of the catalyst is thus correlated with the tube diameter of each CNT. Once laden with the catalyst, the substrate is placed into a tube furnace. The furnace is set to 750°C and ethylene (C_2H_4) gas is flowed into the chamber at a steady rate. The ethylene gas contains the carbon atoms from which the tubes will form. At this elevated temperature, a reaction begins between the ethylene and the metal catalyst, resulting in the growth of the CNTs, perpendicular to the substrate surface. The length of the tubes depends on how long the ethylene gas is flowed. Once the flow is stopped, the reaction ceases. Figure 4 shows the differences in sample appearance before and after the synthesis process. A scanning electron microscope is used to estimate how tall the tubes are. In this study, VACNTs between 100 μm – 140 μm in length are observed with tube diameters of about 4 nm. While they are mostly aligned vertically, on a microscopic scale, it is observed that they can actually be quite curly and sometimes overlap and intertwine. The implications of this on the materials thermal properties will be discussed further in this work.

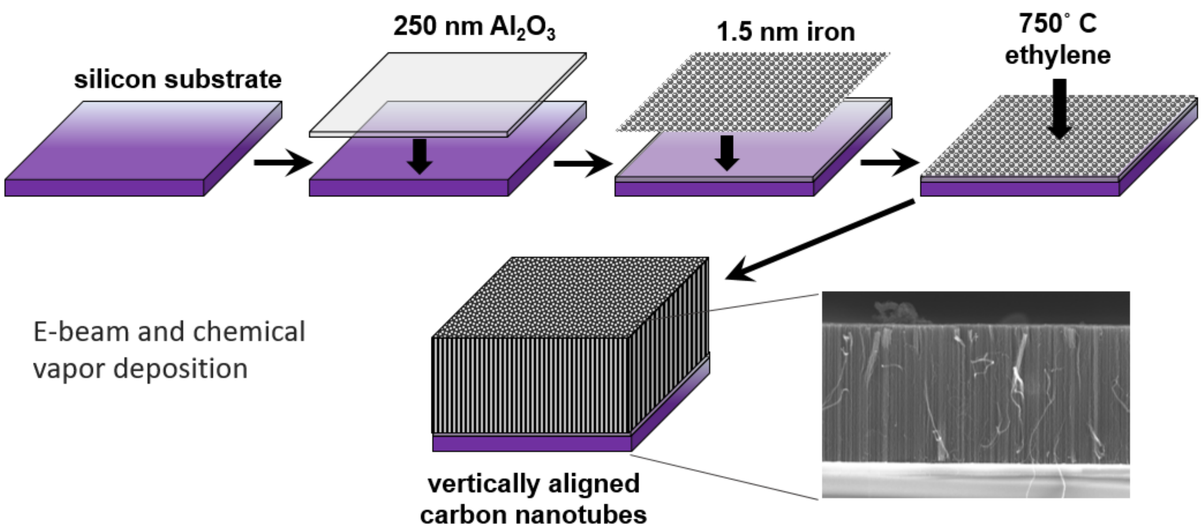

Figure 3. Overview of VACNT growth process [8].

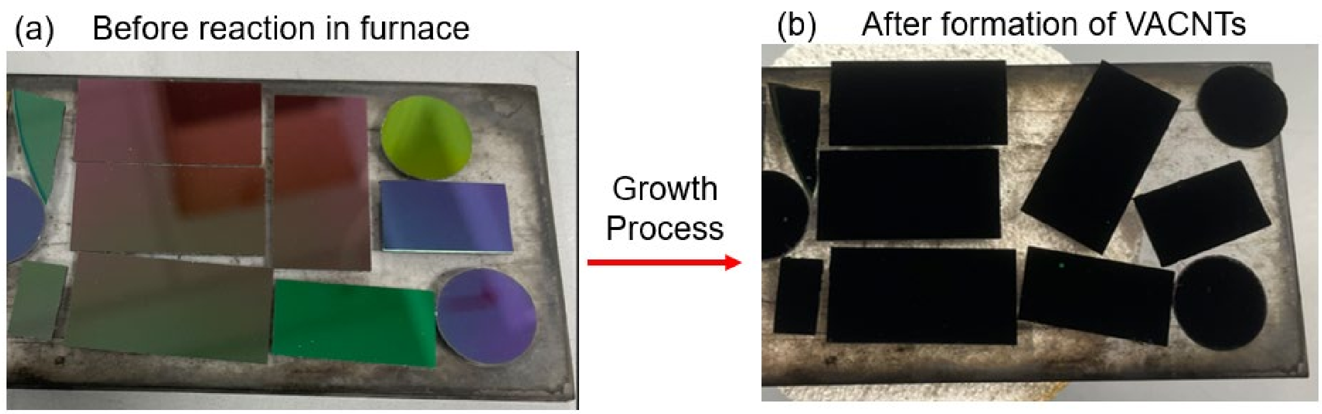

Figure 4. Pictures of substrates before and after VACNT synthesis. The different color substrates in 4(a) indicate different thickness of the buffer layer.

Section 2.2 Optical Properties of VACNTs

When light interacts with a material it can be either reflected, absorbed, or transmitted, with the percentage of each of these cases adding to 100% by conservation of energy. Due to their structure, VACNTs are unique in the sense that almost all incident light energy is absorbed (98% – 99%) over a broad spectrum (0.2µm – 200µm wavelengths) [9]. This is one of the most absorptive materials known to exist. When an object coated in VACNTs is observed, it is extremely difficult to make out its shape, as no light is reflected into the observer's eye. The key characteristics of VACNTs that make this possible are their density, electron band structure, and alignment.

Light travels as waves, consisting of perpendicular, oscillating electric and magnetic fields. These waves travel at the speed of light in vacuum, but slow down if travelling through matter. The ratio of the speed of light in vacuum to the speed of light in a given medium is called index of refraction, n. Index of refraction is related to the material's relative permittivity, ϵ_r, and its relative permeability, μ_r, as shown in equation 1. The descriptor, r, standing for relative, indicates a ratio between the value in vacuum and the value in the material.

$$n = \sqrt{\epsilon_r \mu_r} \qquad (1)$$

Permeability is a measure of magnetization produced in a material in response to an applied magnetic field and is close to 1 for air (μ_r= 1.0000004). Permittivity is a measure of the tendency of a material's atomic charges to change when an electric field is applied. Relative permittivity for air is about 1, resulting in n=1. In low density materials such as VACNTs, electron density is decreased, and therefore permittivity is also decreased.

In materials science, effective medium theory (EMT) is used to approximate bulk properties of composite media. Applying EMT to VACNTs, being a composite material consisting of air and CNTs, an effective dielectric function can be obtained by averaging the electric fields of the two materials. To obtain an effective dielectric function for CNT arrays, the Maxwell Garnett effective medium approximation can be used [10] [11]. These effective values, ϵ_{eff} and μ_{eff}, can then be used in equation 1 to calculate the effective refractive index of VACNT. Due to the spacing between tubes, the index of refraction of VACNT is also close to 1. Figure 5 shows the relationship between VACNT density and index of refraction.

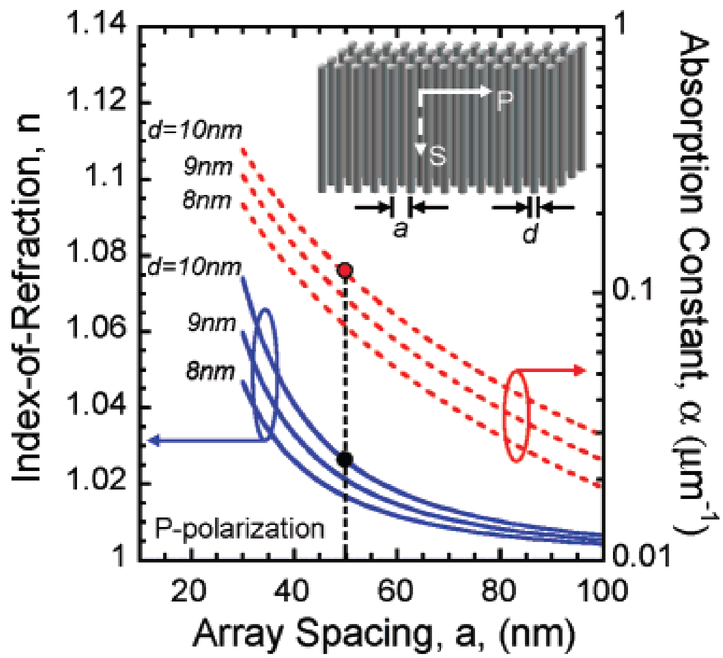

Figure 5. Array spacing vs. index of refraction [12]. As array spacing increases, volume fraction of air increases and the index of refraction of the bulk VACNT approaches 1.

Fresnel's law of reflection, equation 2, states that if the index of refraction between two mediums, n_1 and n_2 are similar, reflectance will be minimized. Figure 6 demonstrates how if the spacing is decreased too much, the reflectance will increase.

$$R = \frac{(n_1 - n_2)^2}{(n_1 + n_2)^2} \qquad (2)$$

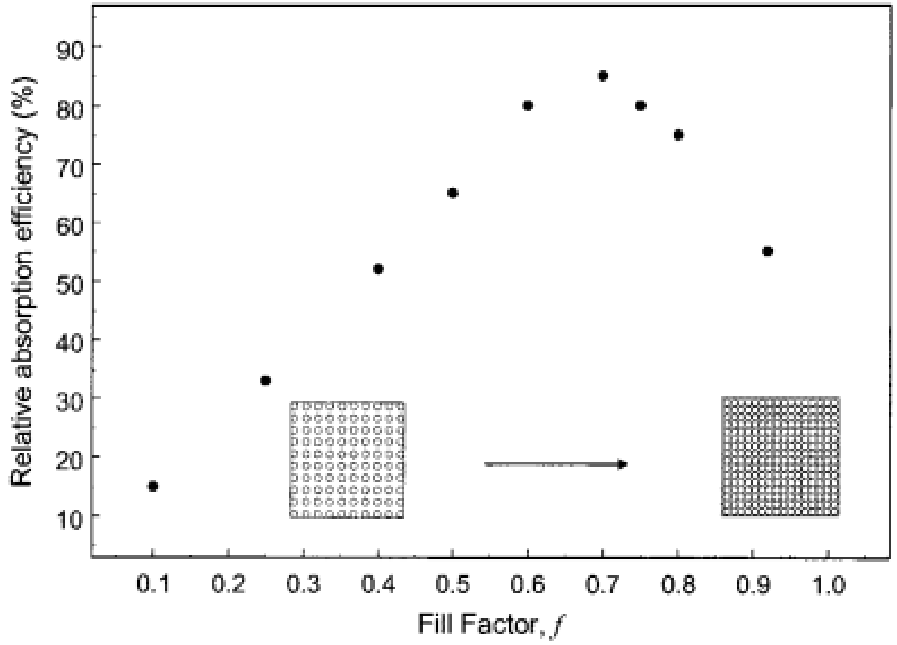

Figure 6. Balance between fill factor (area density) and index of refraction [4]. Greater spacing between tubes decreases absorption, but having tubes touch is also undesirable.

The absorptive qualities of VACNTs are further improved by the alignment of the CNTs. Considering a singular CNT, light that is traveling parallel to the tube axis has minimal interaction with tube (See Figure 7 A). This is because the tube is perpendicular to the light's electric field and so electrons cannot couple with it. As a result, most of the light incident upon the surface enters the material. Due to the imperfect alignment of the tubes and scattering, the light will end up interacting with the sides of the tube, as depicted in Figure 7 B. With each additional interaction, most of the light will be absorbed. This is due to the electronic band structure of the CNTs which leads to high optical absorption [13]. The result of the CNT structure and density is a reflectance <1-2% over 0.2 μm to 200 μm wavelengths. In VACNTs with a high degree of alignment between tubes, reflectance will be increased at normal incidence, but will go down if light comes in at oblique angles.

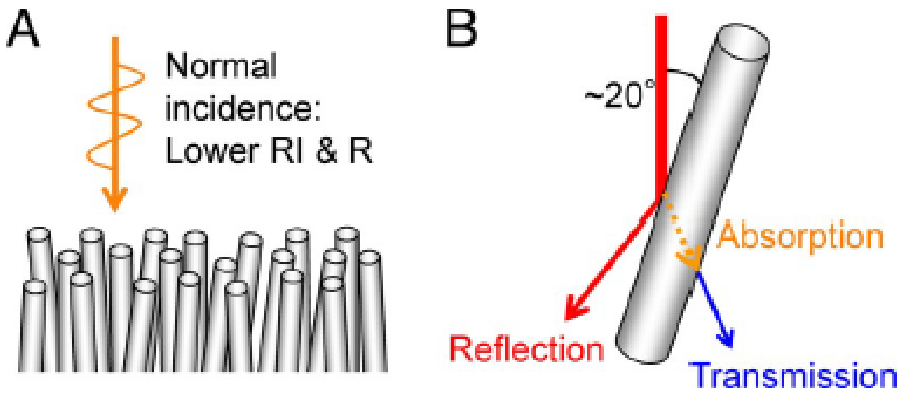

Figure 7. A) Shows how light at normal incidence to a CNT has a perpendicular electric field resulting in a lower RI, refractive index, and R, reflectance. B) Depicts the possible interactions between incident light and a CNT that is slightly angled with respect to that incident light. In this interaction, most of the light is absorbed.

Kirchhoff's law, equation 3, establishes that materials which absorb well must also emit well.

$$A_\lambda = \varepsilon_\lambda \tag{3}$$

Where A is absorptivity and ε is emissivity, both ratios which range from 0 to 1. The subscript indicates that the value can vary for different wavelengths, λ. Absorptivity is the ratio of energy absorbed by a material to the energy incident on the material. Emissivity is the ratio of energy emitted by a material to energy emitted by a blackbody at the same temperature at thermal equilibrium. A blackbody is an ideal material which absorbs 100% of light of every wavelength. Because VACNTs have an extremely high absorptivity, they also have a proportionally high emissivity. VACNTs are one of the closest known existing materials to an ideal blackbody, having an emissivity of 0.98-0.99. Figure 8 compares the emissivity of other high emissivity materials with CNTs.

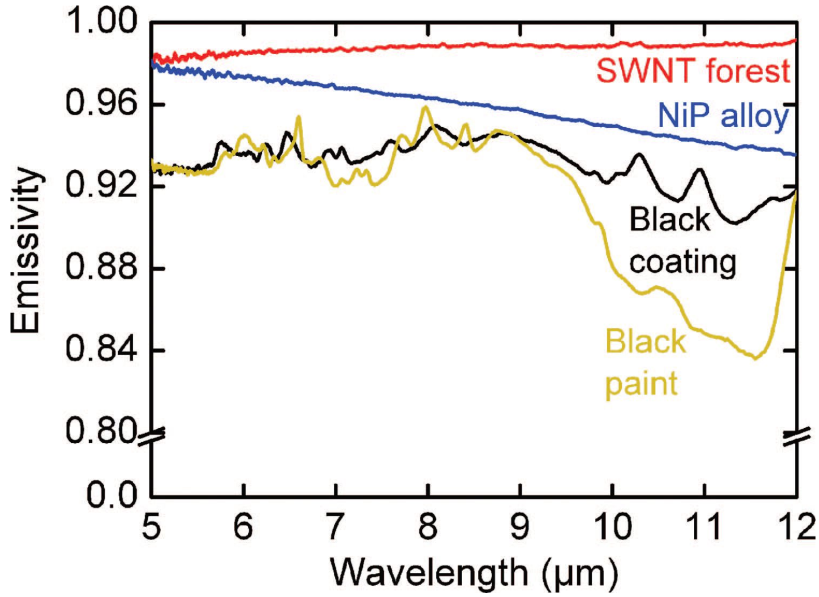

Figure 8. Emissivity of Single Walled Carbon Nanotube (SWNT) forest (red line) compared to other high emissivity materials [9]. SWNT forests, also known as SWCNTs, have similar emissive properties to VACNTs.

Blackbodies emit energy according to Planck's law. Figure 9 shows the spectral radiance of VACNTs as a function of wavenumber closely matching the Planck distribution for a blackbody.

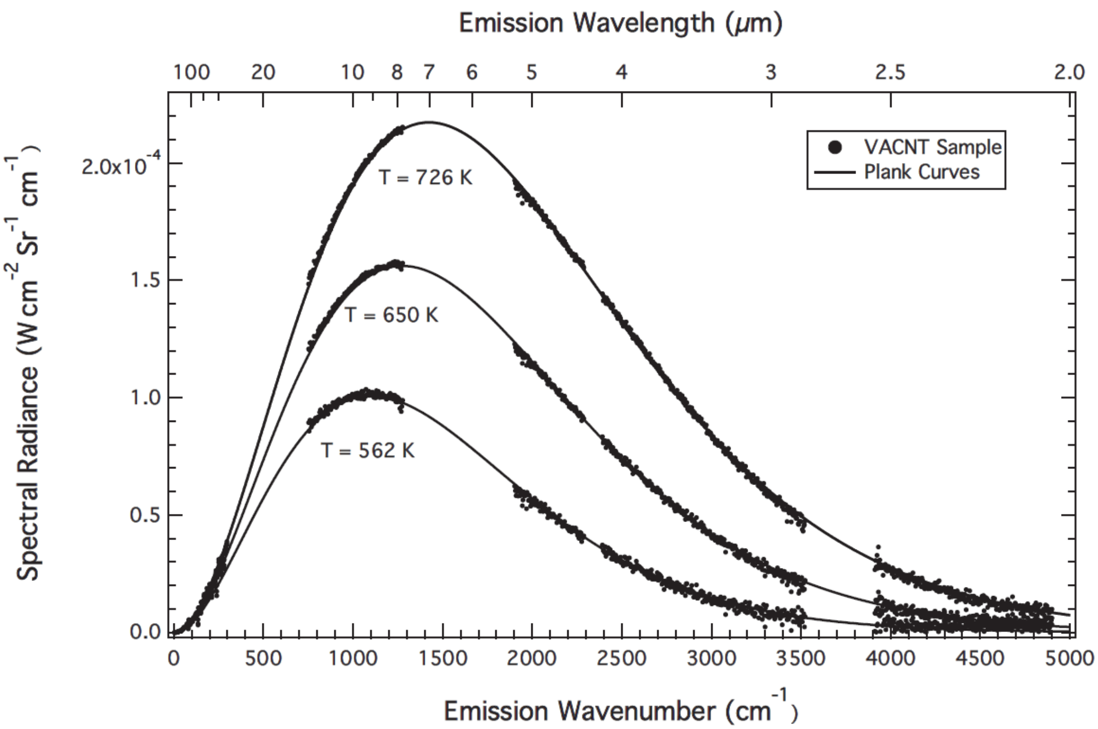

Figure 9. VACNT spectral emission compared to Planck's curve [3]. This data was collected with Fourier transform infrared (FTIR) spectrometer over 3 μm to 13 μm at three different sample temperatures.

Blackbodies, being Lambertian, emit this radiation in every direction equally as stated in Lambert's cosine law. While the emitted power from a given area on a Lambertian surface drops off by the cosine of the emission angle relative to surface normal, the solid angle subtended by surface area visible to the viewer is reduced at the same rate. The result is the surface looking equally bright from any direction. A bidirectional reflectance distribution function (BRDF) defines how light is reflected off a material and is a function of incidence angle, and reflectance angle. Figure 10 shows the BRDF of a VACNT sample matching closely with a theoretical Lambertian surface. The deviation from the theoretical curve at reflectance angles of -20 degrees and +20 degrees can be attributed to the geometry of the set up that was used to collect the data. At -20 degrees, the detector is blocking the incident beam. At +20 degrees, the specular reflection is due to partially coherent scatter [3].

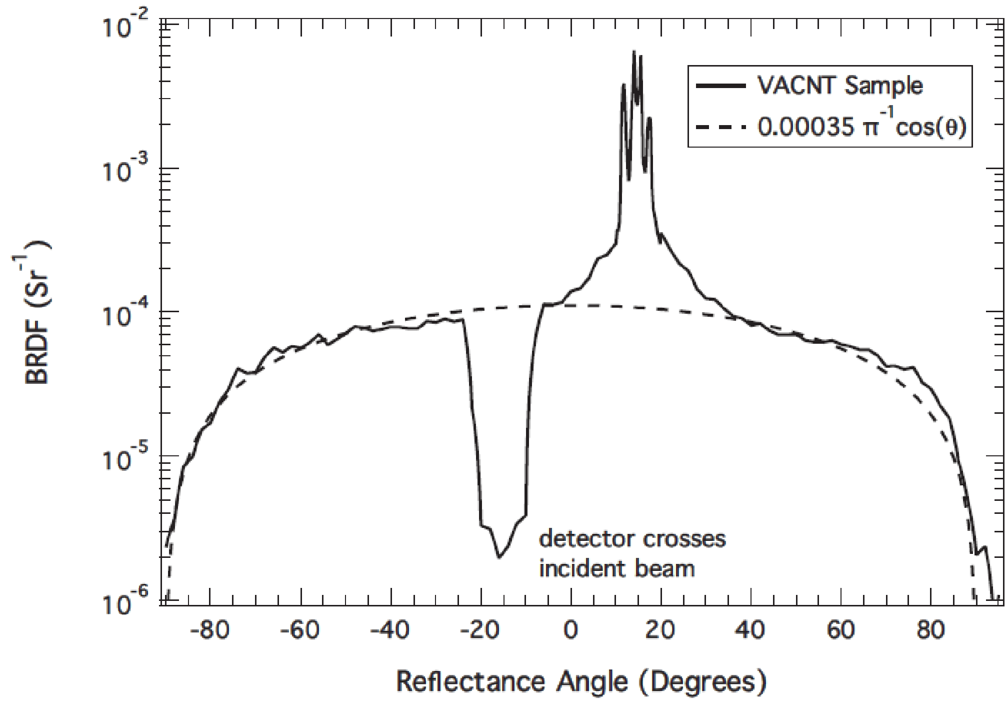

Figure 10. Bidirectional Reflection Distribution Function (BRDF) of a perfect Lambertian surface (dotted line) compared to BRDF of VACNTs (solid line) [3].

Section 2.3 Thermal Properties of VACNTs

In addition to having very unique optical properties, VACNTs also have interesting thermal properties. Similar to how photons are quantized particles of light waves, phonons are quantized particles of sound waves. Phonons provide heat transport within a medium. The reason carbon nanotubes are extremely good conductors along the tube axis, in the axial direction, is due to a high mean free path of phonons. This refers to how far phonons can travel without interruption. Perpendicular to the tube axis, the mean free path of phonons is much lower, resulting in good thermal insulation in this direction [1]. When arranged in a tube forest, the properties of a singular CNT, as described in chapter 1, are not retained. Due to entanglement of neighboring fibers, the phonon mean free path in the axial direction decreases. Additionally, impurities and misalignments can degrade thermal properties further [14]. Instead, thermal conductivity along the tube axis reaches up to 1500 W/m*K [15]. Assemblies, however, are still fairly anisotropic, with thermal conductivity perpendicular to the tube axis of around 0.1 W/m*K [16].

Chapter 3: Motivation and Goal

It has been shown that the thermal and optical properties of the material can vary depending on synthesis parameters. For example, if VACNTs are grown too dense, or the degree of alignment of tubes is too high, their bulk reflectance can increase, as described in Chapter 2. Additionally, it has been shown that there is a correlation between thermal conductivity and tube length [17] [18]. Thus, to ensure optimum traits are retained, it is important to be able to measure their final properties. Furthermore, having a measurement capability enables the synthesis process to be fined-tuned and tailored to specific applications. In applications where insulation between tubes is of high importance, measurement of thermal diffusivity is critical.

Thermal diffusivity, α, having units of cm^2/s, is a measure of how fast heat moves within a material. It depends on thermal conductivity (W/m*K), k, density (kg/m^3), ρ, and specific heat (J/(kg*K), c_p, as shown in equation 4.

$$\alpha = \frac{k}{\rho * c_p} \tag{4}$$

It is typically measured for isotropic materials using a method called Laser Flash Analysis (LFA). This technique measures how long it takes for heat to transfer from the front surface to the back surface of a material. The front side is illuminated with a light source and the temperature signal in time is captured from the backside, as depicted in Figure 11. This works well for isotropic materials, but does require access to both the front and back side of the sample, which is not always possible. Since VACNTs are anisotropic, having a different thermal diffusivity in the two axes, the LFA method is not sufficient to provide a measurement in the transverse direction, the axis perpendicular to the tube alignment direction. Furthermore, the measurement would need to isolate thermal diffusivity of the CNTs from the substrate's thermal diffusivity.

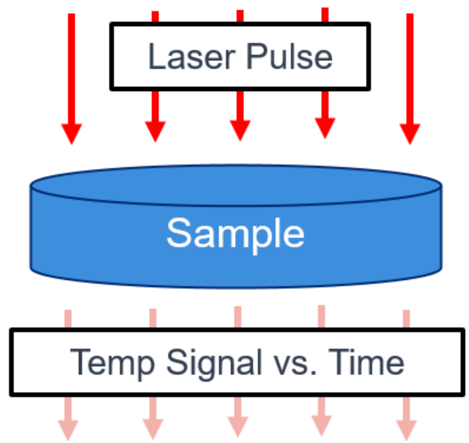

Figure 11. LFA diagram.

There are alternative methods to measure the thermal diffusivity in the VACNTs' transverse direction. In one case, Ivanov and colleagues. grew tubes to more than 2 mm in length, removed them from the substrate with a razor blade, and used a laser pulse perpendicular to the tube axis. Here the tubes are long enough for a laser spot to hit one side and measure heat on the other side [19]. However, this poses challenges for tubes lengths on the order of microns. In work done by Cohen et. al., a VACNT array is heated from the substrate and the system is imaged with an infrared (IR) camera from the side [20]. That paper studies how VACNTs dissipate heat but does not report quantitative transverse thermal diffusivity measurements. Here they find that shorter VACNTs conduct heat along the axial direction with negligible convection from the sidewalls. In a third source, Borca-Tasciuc et. al. compare two methods of measuring VACNT thermal diffusivity [14]. In one method, a laser illuminates the VACNT surface and the back surface temperature of the sample is measured with thermocouples. The transverse thermal diffusivity is not measured directly, but is rather calculated from the measured axial thermal diffusivity. They find these results have good agreement with measurement of the thermal diffusivity in the axial direction using a "self-heating 3ω" technique, but again this does not directly measure the value in transverse direction. So, for short tubes, on the order of 100um, there is a gap in the literature for direct measurement of the transverse thermal diffusivity. Also, in general, there is more literature on thermal conductivity rather than thermal diffusivity.

For other anisotropic materials, multiple sources have used methods of experimentally measuring thermal diffusivity in the transverse direction via IR thermography [21] [22] [23]. In that method, a Gaussian laser pulse is used to heat the surface instantaneously. An IR camera images the front surface of the material to capture the spot size as it spreads out spatially in time. These references provide derivations that begin with the heat equation and the initial laser parameters and result in a relationship between thermal diffusivity and the growth rate of the spot size. This relationship is outlined in equation 5 [21].

$$b_i^2 = a^2 + 8D_i t \tag{5}$$

Where b_i is the measured radius of the Gaussian spot, a is the initial beam radius, D_i is the thermal diffusivity, and t is the time after laser pulse. By plotting the Gaussian radius squared as a function of time after laser pulse and fitting a straight line to the data, the slope is equal to 8 times the thermal diffusivity of the material. This technique has been experimentally verified to match theoretical relationships for both isotropic and anisotropic materials and is also independent of initial spot size that is used.

The goal of this work is the application of short pulse illumination with IR camera capture for transverse thermal diffusivity measurement for VACNT arrays. This technique has not yet been utilized to measure the transverse thermal diffusivity of VACNT arrays. An experimental setup was established to achieve this and MATLAB scripts were created to analyze the collected data. This report discusses the results, as well as recommendations on future experiments in order to more completely characterize heat transport within VACNT arrays.

Chapter 4: Experimental Description

An overview of the experimental setup is shown in Figure 12. The illumination source used was a Photonics Industries 1064 nm pulsed laser set to 10 ns pulse width at 100Hz repetition rate and 50A current. These settings produced about 0.7 mJ of pulse energy at the sample, verified by an Ophir PE50-DIF-ER-C pulsed energy meter. The VACNT samples were placed about 4 ft from the output of the laser.

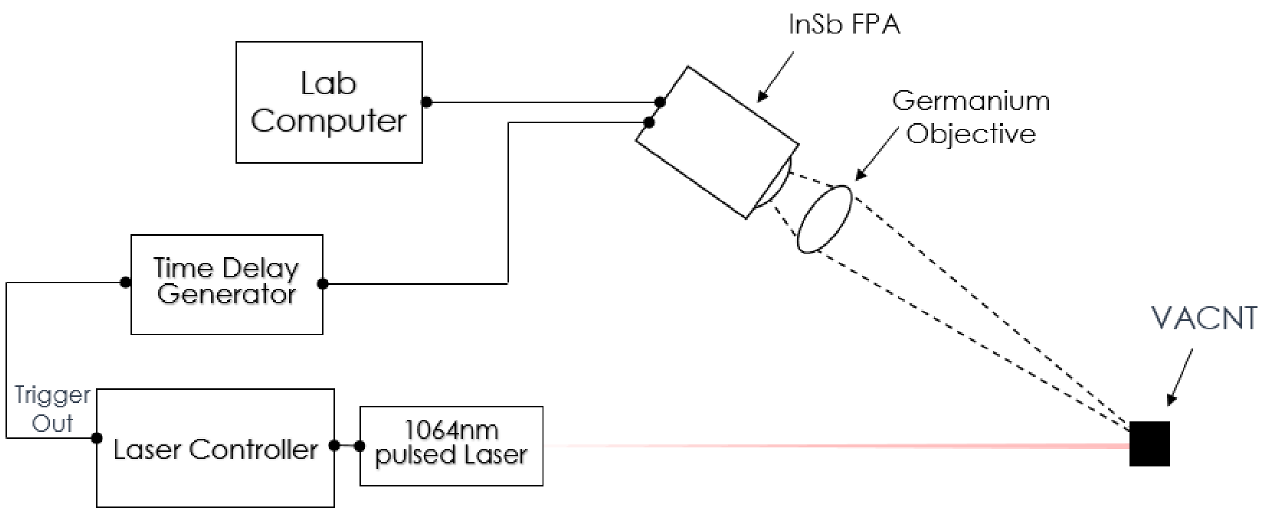

Figure 12. Schematic of experimental setup.

The samples were mounted such that the long axis of the tubes was parallel with the incoming laser beam. The samples were held in the mount by the edges of the substrate. The dimensions of VACNT samples were 2 cm x 2 cm. The laser $1/e^2$ spot diameter incident on the VACNT sample was 2.1 mm. This was validated by placing a beam profiler (Ophir LT665) at the location of the sample. Figure 13 shows the output of the profiler right after the aperture and after it propagated to the plane of the VACNT sample.

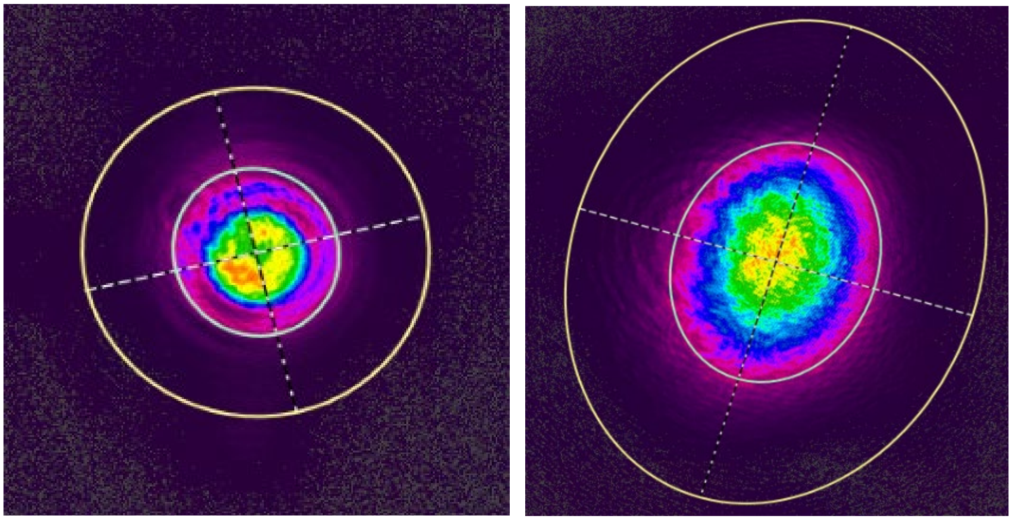

Figure 13. Beam profile of pulsed laser, at laser aperture, left, and after propagation to the sample plane, right.

The IR emission of the VACNT, as it absorbed the energy of the laser, was captured with a Telops MS M1K infrared camera using a cooled InSb, 640 x 512 detector, with a pixel pitch of 25 µm, sensitive between 1.5 µm – 5 µm wavelengths. The calibrated camera data has a temperature accuracy of 2 K and 14 bits of dynamic range. The VACNT sample was angled normal to the camera's optical axis. Due to this viewing geometry, the laser beam was incident off normal and slightly stretched in the horizontal direction, but able to be uniformly focused on by the camera. A f/2.5 lens with an effective focal length of 100 mm was mounted to the Telops camera. An external germanium-silicon relay was used to increase spatial resolution. The relay is a triplet f/6.14 lens with an effective focal length of 312 mm. Due to the transmission spectrum of germanium, the 1µm laser wavelength was blocked from the detector. This isolates the radiation of the CNTs caused by the absorption of the lasers' energy. The spatial resolution of measurement is 67 µm per pixel. This was verified by placing an object of known size, a Thorlabs BHM3 ruler, in focus at the image plane. Figure 14 shows an image of the ruler at the focal plane. The tic marks are separated by 1 mm. ImageJ, image analysis software, was used to measure the number of pixels spanning 10 mm.

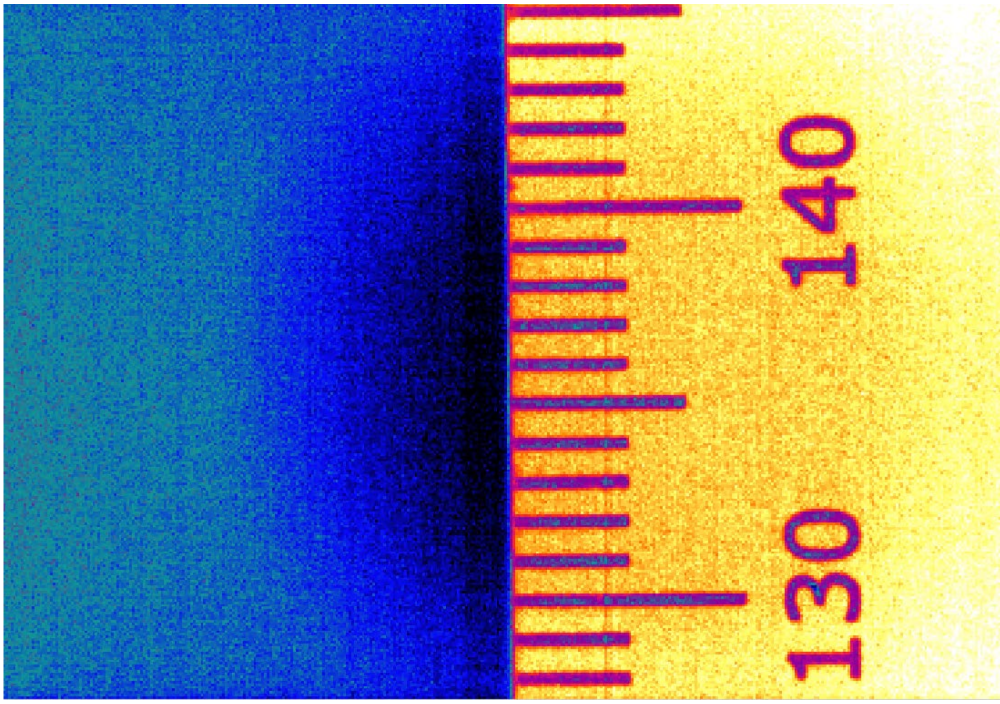

Figure 14. Image of Thorlabs ruler (part number BHM3) used to calculate spatial resolution.

In the experiment, image capture was triggered by the pulse of the laser and collected via the Telops interface software. The integration time of the camera was set to 10 μs. Before data collection began, a single temperature point pixel non-uniformity correction (NUC) was performed at ambient conditions (~25°C) by covering the camera with its lens cap.

A Stanford Research Systems DG645 delay generator was placed in line with the trigger from the laser to the camera. This was done so that the 2D thermal signature could be captured at various times after the laser pulse to investigate the thermal decay of the VACNT sample. To capture the thermal signature at the time of the pulse, the delay generator was set to a delay of 0 μs. Delays were introduced in increments of 10 μs up to 100 μs. One hundred images were captured at each time delay and averaged for analysis. The integration time needed to be long enough for a sufficient signal to noise ratio and short enough to have good temporal resolution.

It was experimentally verified that the heat signature on the surface of the VACNT completely decays to the same temperature as the substrate by 1 ms after the laser pulse, and the signal is reduced by 90% at 250 µs after the pulse. Since the rep rate of the laser was set to 100 Hz, the time between pulses was 10 ms. Thus, it was confirmed that over time, the sample was not heating up and each pulse could be considered independent.

The camera and lens assembly were calibrated with a small aperture (4 mm) cavity blackbody placed at the sample plane in order to obtain a relationship between counts and blackbody temperature. The raw data were analyzed by selecting a region of interest within the cavity and taking the mean digital counts within this area. The raw data were fit to a 5^{th} order polynomial, which is shown as the red line in Figure 15. A lookup table was then generated to convert from camera counts to temperature.

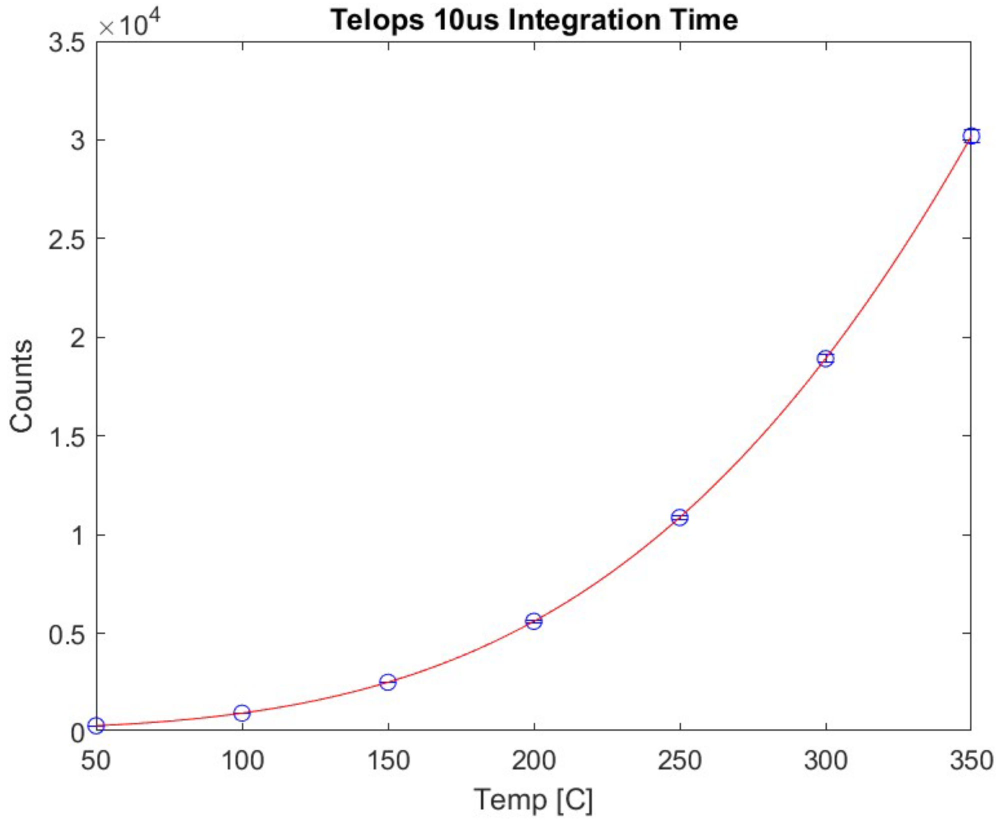

Figure 15. Blackbody temperature vs. digital counts.

Chapter 5: Data Analysis Process

The process to obtain the thermal diffusivity value is described as follows. The raw Telops data is processed using MATLAB to obtain a temperature image. For each time delay, the 100 captured images are averaged to form a single image. This results in 11 images for each sample, corresponding to the 11 time delays since laser pulse (0 – 100μs in 10μs increments). An example of a cropped image at time t = 0 μs is shown in Figure 16. The peak temperature in the center is 244°C.

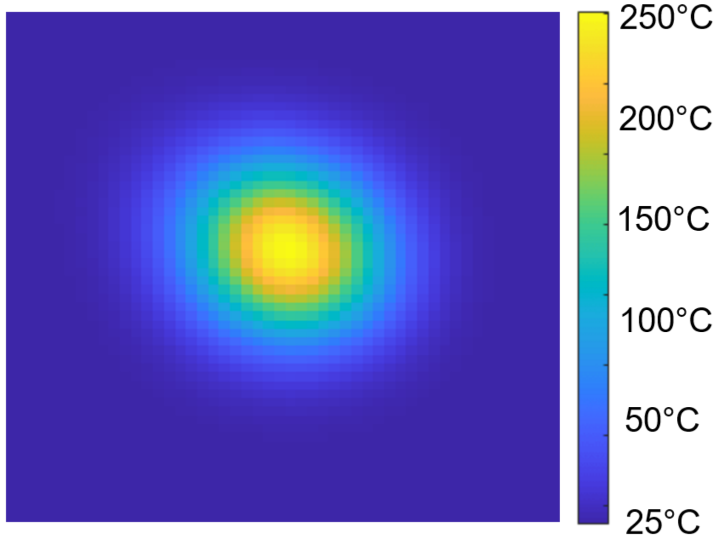

Figure 16. Intensity profile of VACNT at t = 100 μs.

The pixel coordinates of the center of the Gaussian spot are found using a centroiding function. For each time delay, a line cut at the centroid location is taken in both the horizontal and vertical directions, and each are separately fit to the equation for a Gaussian function shown in equation 6.

$$f(x) = a\exp\left(-\frac{(x-b)^2}{2c^2}\right) \qquad (6)$$

Where a is the amplitude, b is the position of the center, and c is the standard deviation, or radius of the Gaussian function.

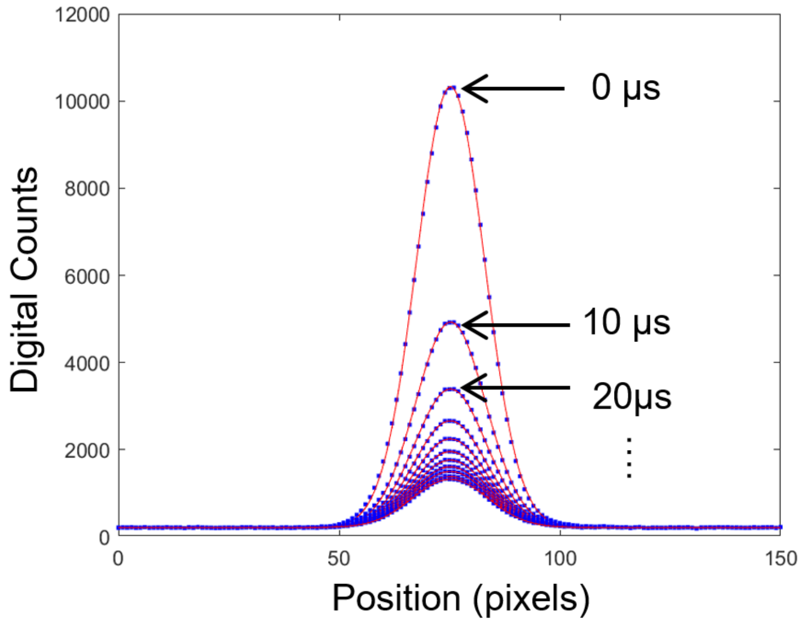

Figure 17. Line cuts through the spot at each time delay. Red line is the fit to raw data points, blue.

The r-squared value for each of these fits was always greater than .98. The fitted Gaussian width parameter, c in equation 6, is stored for each time delay. Since these values are in units of pixels, it is necessary to use the spatial calibration (67 μm per 1 pixel) to convert to units of centimeters. Plotted in Figure 18 as the blue circles are the square of the radii at each time delay. A linear fit is performed on this data. The slope of this line is then divided by 8, and the value for thermal diffusivity is obtained per equation 6.

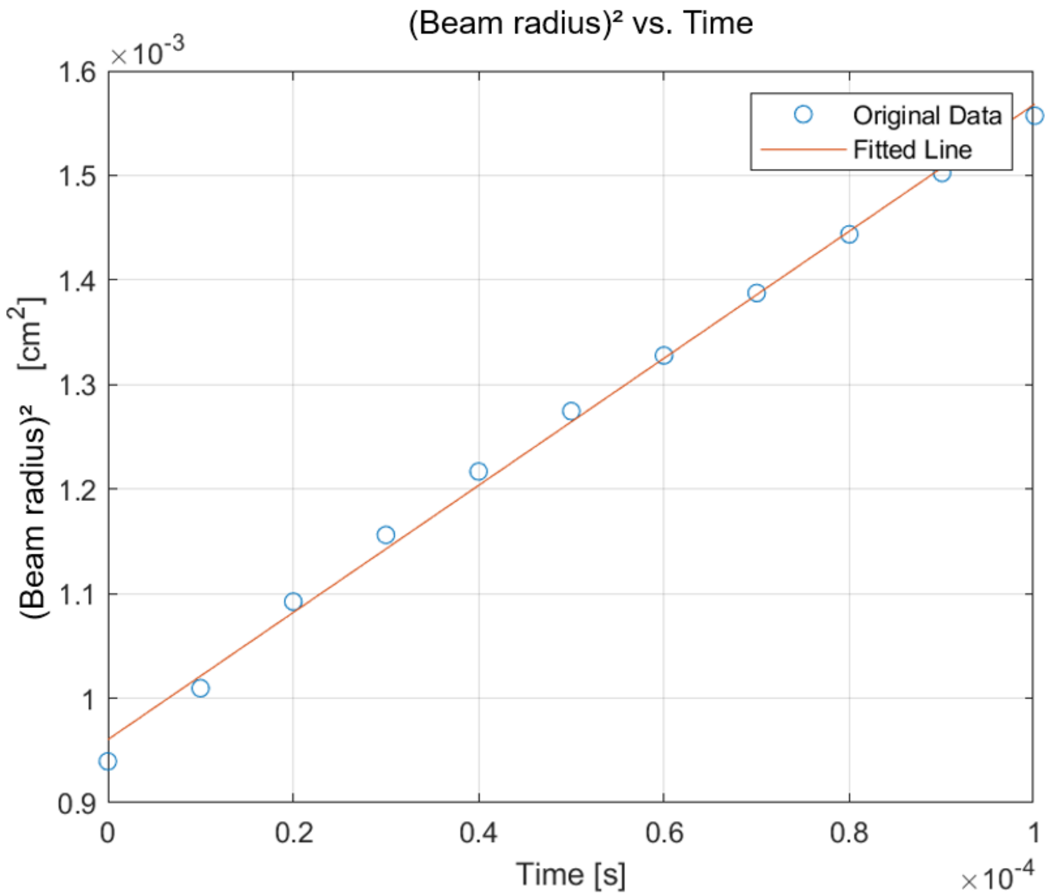

Figure 18. Beam radius squared vs. time. Slope of regression line equal to 8 times the thermal diffusivity.

The main source of uncertainty in this value is the fit confidence of the linear relationship. Slightly different slope values are obtained whether line cuts are taken in the horizontal or vertical direction. Because this method is independent of spot size, the difference is probably not attributed to ellipticity in the beam, as the respective directions should be spreading out at the same rate, but rather variations in the sample. For the reported thermal diffusivity value, an average was taken of the results from the horizontal and vertical directions. The reported error in this value is the standard deviation between the two calculations. The quality of the Gaussian fit is very important to this measurement. A poor fit could yield an incorrect beam radius and therefore slope. Having sufficient spatial resolution, i.e. enough data points across the Gaussian profile, is therefore important for the fit.

Repeatability uncertainty of the measurement was also investigated. Without moving the sample or laser illumination location, each dataset (recording of 100 images at each delay time) was repeated three times. The analysis of each dataset yielded almost the exact same thermal diffusivity value. This agrees with the standard deviation across the collected images for each time delay being very small. Thus, there is confidence that the measurement itself is stable.

Chapter 6: Thermal Diffusivity Results and Discussion

Reported here are the thermal diffusivity values calculated for three different VACNT samples. The samples were prepared in the same way except the amount of time the seed gas, ethylene, was flowed in the furnace varied between 5, 6, and 8 minutes. Tube length is linear with growth time, so this resulted in each sample having a successively longer length: 103 µm, 114 µm, and 136 µm. Figure 19 shows how longer growth times can lead to increased tortuosity, or "curliness".

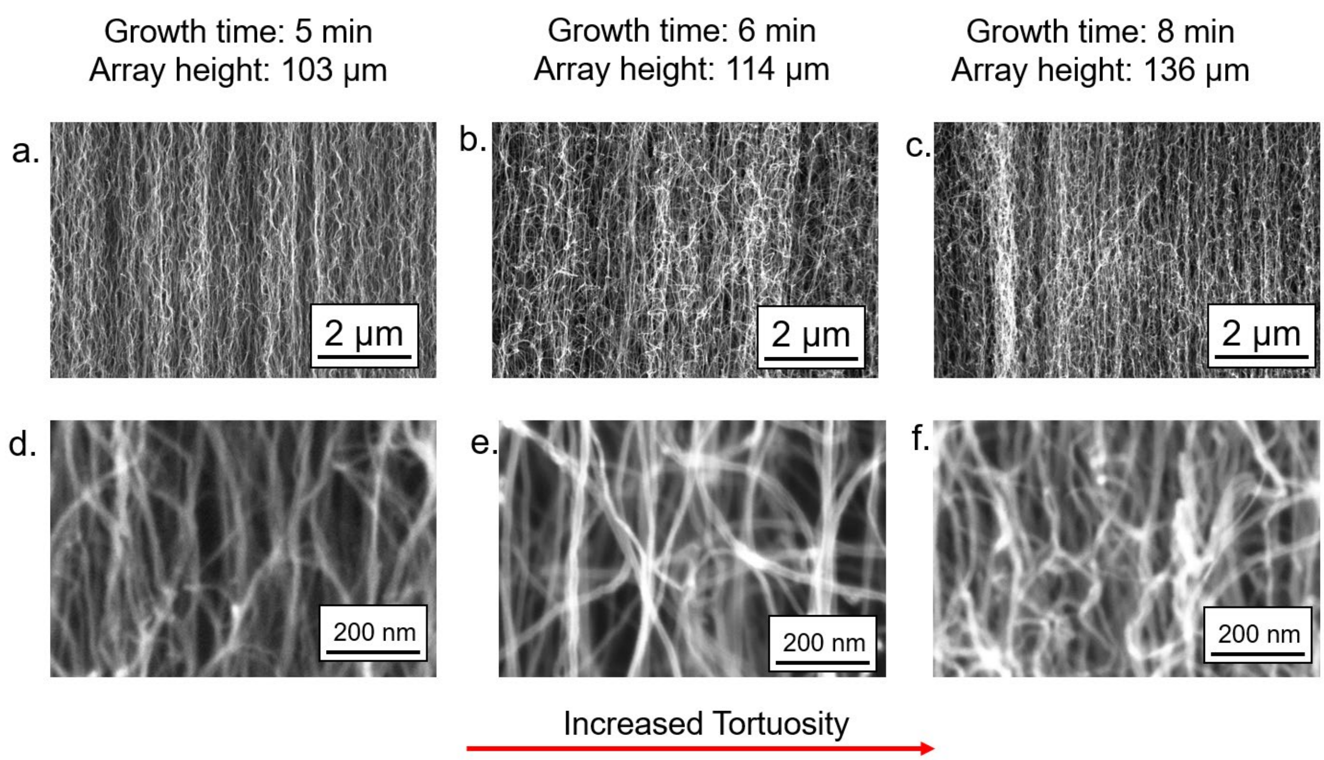

Figure 19. SEM images of the three samples measured in this work, viewed from the side, at 2 different scales. The tubes appear straighter and less dense in 19d., a 5-minute growth, than the tubes in 19f., an 8-minute growth.

Figure 20 shows the calculated transverse thermal diffusivity values calculated for each sample plotted against growth time.

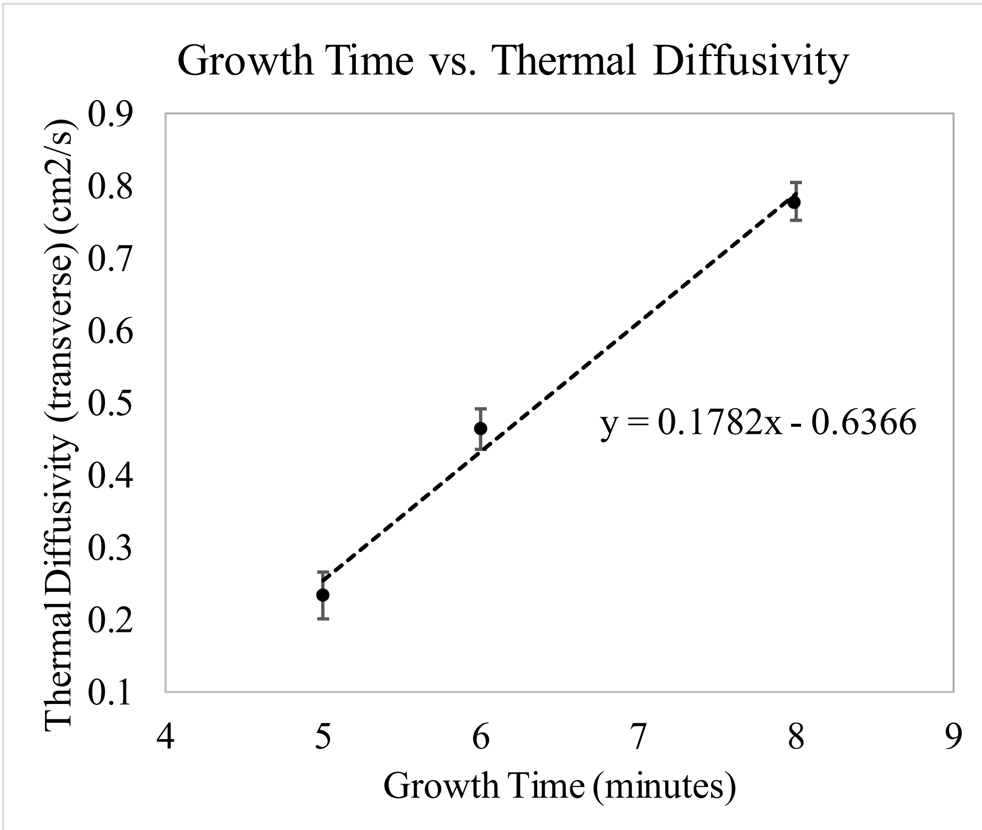

Figure 20. Thermal diffusivity values for three different VACNT samples.

The trend of the data suggests that longer growth time is linearly correlated with a higher transverse thermal diffusivity value. This trend agrees with statements in literature describing longer tube lengths, produced by longer growth times, providing more pathways for heat transport [19] [24] [25] [26]. This trend is supported by qualitative analysis of the SEM images in Figure 19. Longer growth times appear to produce CNTs with increased density and tortuosity. As density of the material increases, thermal conductivity, and therefore thermal diffusivity, would also increase. The increase in tortuosity indicates the phonon mean free path in the transverse direction has also increased, further supporting an increase in transverse thermal diffusivity. For a more quantitative analysis, the density of the samples could be measured by weighing the samples before and after VACNT growth. Also, the degree of tube alignment in each sample could be measured via X-ray diffraction [27].

When compared to other reported values of VACNT thermal diffusivity in transverse direction, these values appear to be higher. Values in literature range from 0.01 cm^2/sec to 0.25cm^2/sec [19] [14]. This work measures values of 0.23 ± 0.032 cm^2/sec, 0.46 ± 0.028 cm^2/sec, and 0.78 ± 0.026 cm^2/sec. This variation could be due to numerous factors. For instance, differences in the synthesis process might yield a different final structure of the VACNTs and thus thermal properties could be vastly different. It is recommended that future studies are performed to measure thermal conductivity, density, and specific heat to verify this. Additionally, calibrating the system with a known material would also reduce uncertainty in the measurements. The latter method was attempted, but most materials are not as absorptive as VACNTs, requiring much higher powers or higher pulse repetition rates in order to get a good signal. The studies that apply this measurement method use pulse energies up to 25J to test metals, rather than 0.7 mJ per pulse used here. The risk of stray reflections is also increased since a higher percentage of the light is reflected with poorer absorbers. One of the materials on which this measurement was attempted was aluminum coated in Aeroglaze Z306, a common coating used in aerospace applications. An energy density high enough to capture data with a good enough signal to noise ratio was unable to be produced with this laser. A future study could employ a higher power laser and increased laser safety measures in order to collect quality data.

A brief investigation was conducted in the physics modelling software, COMSOL, to simulate this experiment. A model was created of the VACNT as a bulk anisotropic material, and an initial Gaussian temperature profile as a boundary condition on the surface. The model outputs were the spatial temperature on the surface in time which could then be analyzed with the MATLAB scripts. However, with only rough estimation of density, specific heat, and thermal conductivity, the results could not be compared with the experimental results. Once future work is performed that measures these parameters, this model can be completed.

There are improvements that could be made to this experiment and analysis. For example, instead of taking a 1D slice through the Gaussian spot, a 2D Gaussian equation could be fit to the data. Alternatively, a radial average of 1D slices could be performed before the fit. It would be interesting to see how these methods compare to each other and to the analysis performed in this work. In this experiment, it was found that having sufficient spatial resolution was important to having enough data points for a satisfactory fit. Having higher spatial resolution results in more data points along the 1D spot, which could improve accuracy. Also, there could be alternative methods for measurement of the spot size from the thermographic data. Instead of taking the standard deviation of Gaussian fit, one might try to measure the full-width at half-maximum (FWHM). However, the points between neighboring pixels would need to be interpolated or else there might be more error due to rounding to the nearest pixel location.

Thermal diffusivity is a property that can change with temperature. In future work, it would be interesting to map out this relationship for VACNT arrays. In this work, only one location on the array was evaluated. For practical applications, VACNTs would need to be investigated for uniformity. Furthermore, the data collected in this work could be analyzed in a different way to extract the axial thermal diffusivity [21].

Chapter 7: Summary

A test setup has been established to investigate heat transport within vertically aligned carbon nanotube (VACNT) arrays. A method for measurement of transverse thermal diffusivity via IR thermography has been demonstrated with VACNT arrays. The trend of the results indicating that longer VACNT lengths are correlated with increased transverse thermal diffusivity is consistent with previous work. The measured thermal diffusivities in the transverse direction of the VACNTs, ranging from 0.23 cm^2/sec to 0.77 cm^2/sec, are on the higher end of values reported in the literature. Additional measurements and calibration would help verify these results and validate the test methods used to obtain them. Recommendations for future work include measurements of the other properties related to thermal diffusivity, measurement of the degree of alignment of the tubes, and measurement of the uniformity of the samples. Compared to other methods of measuring transverse thermal diffusivity of VACNT arrays, the approach used here only requires access to the front side of the sample. Additionally, in applications where heat transport on the front surface is critical, this method gives a direct measurement rather than calculating it from other measurements. This method has potential to further the understanding of heat transport within VACNT arrays and address a critical need to provide assessment of thermal performance for feedback to the synthesis process.

REFERENCES

[1] P. Kim, "Thermal Transport Measurements of Individual Multiwalled Nanotubes," Phys. Rev. Lett., p. 87 (21), 2001.

[2] S. Sinha, S. Barjami, G. Iannacchione, A. Schwab and G. Muench, "Off-axis thermal properties of carbon nanotube films," Journal of Nanoparticle Research, vol. 7, pp. 651-657, 2005.

[3] R. Fainchtein, D. M. Brown, K. M. Siegrist and A. H. Monica, "Time-dependent near-blackbody thermal emission from pulsed laser irradiated vertically aligned carbon nanotube arrays," Phys. Rev. B, vol. 85, no. 12, 2012.

[4] E. Theocharous, "Evaluation of a pyroelectric detector with a carbon multiwalled nanotube black coating in the infrared," Applied Optics, vol. 45, no. 6, pp. 1093-1097, 2006.

[5] A. Cao, Z. Xianfeng, C. Xu, B. Wei and D. Wu, "Tandem structure of aligned carbon nanotubes on Au and its solar thermal absorption," Solar Energy Materials and Solar Cells, vol. 70, no. 4, pp. 481-486, 2001.

[6] C. Granqvist, "Radiative Heating and Cooling with Spectrally Selective Surfaces," Applied Optics, vol. 20, pp. 2606-2615, 1981.

[7] V. Foldyna, J. Foldyna and M. Zelenak, "Dispersion of carbon nanotubes for application in cement composites," Procedia Engineering, vol. 149, pp. 94-99, 2016.

[8] A. G. Simmonds, Artist, [Art]. Johns Hopkins University Applied Physics Lab, 2024.

[9] K. Mizuno, J. Ishii, H. Kishida and Y. Hayamizu, "A black body absorber from vertically aligned single-walled carbon nanotubes," Proceedings of the National Academy of Sciences, vol. 106, no. 15, pp. 6044-7, 2009.

[10] F. Garcia-Vidal, "Effective Medium Theory of the Optical Properties of Aligned Carbon Nanotubes," Physics Review Letters, vol. 78, no. 22, pp. 4289-4292, 1997.

[11] J. Lehman, N. Tomlin, D. Conklin and M. Stephens, "Carbon nanotube-based black coatings," Applied Physics Reviews, vol. 5, pp. 011103-17, 2018.

[12] Z.-P. Yang, L. Ci, J. A. Bur, S.-Y. Lin and P. M. Ajayan, "Experimental Observation of an Extremely Dark Material Made By a Low-Density Nanotube Array," Nano Letters, vol. 8, no. 2, pp. 446-451, 2008.

[13] G. Ho, Y. Ho, T. Li, C. Chang and M. Lin, "Band structure and absorption spectrum of double-walled zigzag carbon nanotubes in an electric field," Carbon, vol. 44, no. 11, pp. 2323-2329, 2006.

[14] T. Borca-Tasciuc, S. Vafaei, D.-A. Borca-Tasciuc, B. Q. Wei, R. Vajtai and P. M. Ajayan, "Anisotropic thermal diffusivity of aligned multiwall carbon nanotube arrays," Journal of Applied Physics, vol. 98, no. 054309, 2005.

[15] K. K. Koxiol, D. Janas, E. Brown and L. Hao, "Thermal properties of continuously spun carbon nanotube fibres," Physica E: Low-dimensional Systems and Nanostructures, vol. 88, pp. 104-108, 2017.

[16] B. Kumanek and D. Janas, "Thermal conductivity of carbon nanotube networks: a review," Journal of Materials Science, vol. 54, pp. 7397-7427, 2019.

[17] L. Qiu, X. Wang, G. Su, D. Tang, X. Zheng, J. Zhu, Z. Wang, P. M. Norris, P. D. Bradford and Y. Zhu, "Remarkably enhanced thermal transport based on a flexible horizontally-aligned carbon nanotube array film," Scientific Reports, vol. 6, no. 21014, 2016.

[18] J. Che, T. Cagin and W. A. Goddard III, "Thermal conductivity of carbon nanotubes," Nanotechnology, vol. 11, pp. 65-69, 2000.

[19] I. Ivanov, "Fast and highly anisotropic thermal transport through vertically aligned carbon nanotube arrays," Appl. Phys. Lett., vol. 89, no. 223110, 2006.

[20] Y. Cohen, S. K. Reddy, Y. Ben-Shimon and A. Ya'akobovitz, "Height and morphology dependent heat dissipation of vertically aligned carbon nanotubes," Nanotechnology, vol. 30, no. 505705, 2019.

[21] N. W. Pech-May, A. Mendioroz and A. Salazar, "Simultaneous measurement of the in-plane and in-depth thermal diffusivity of solids using pulsed infrared thermography with focused illumination," NDT & E International, vol. 77, pp. 28-34, 2016.

[22] Y. Zhang, R. Xu, Y. Liu, Q. Jiang, Q. Li, Y. Liu and J. Wang, "Anisotropic thermal diffusivity measurement of thin films: From a few to hundreds of microns," International Journal of Heat and Mass Transfer, vol. 227, no. 125536, 2024.

[23] F. Cernuschi, A. Russo, L. Lorenzoni and A. Figari, "In-plane thermal diffusivity evaluation by infrared thermography," Review of Scientific Instruments, vol. 72, pp. 3988-3995, 2001.

[24] M. B. Jakubinek, M. A. White, G. Li, C. Jayasinghe, W. Cho, M. J. Schulz and V. Shanov, "Thermal and electrical conductivity of tall, vertically aligned carbon nanotube arrays," Carbon, vol. 48, no. 13, pp. 3947-3952, 2010.

[25] H. Xie, A. Cai and X. Wang, "Thermal diffusivity and conductivity of multiwalled carbon nanotube arrays," Physics Letters A, vol. 369, no. 1-2, pp. 120-123, 2007.

[26] P. Ebin and J. S. Babu, "Effects of length, diameter, and doping on the thermal transport in carbon nanotubes: a molecular dynamics study," Applied Nanoscience, vol. 14, no. 2, pp. 339-351, 2023.

[27] A. Cao, C. Xu, J. Liang, D. Wu and B. Wei, "X-ray diffraction characterization on the alignment degree of carbon nanotubes," Chemical Physics Letters, vol. 344, no. 1-2, pp. 13-17, 2001.

[28] C. Cheng, W. Fan, J. Cao, S.-G. Ryu, J. Ji, C. P. Grigoropoulos and J. Wu, "Heat Transfer across the Interface between Nanoscale Solids and Gas," American Chemical Soceity, vol. 5, no. 12, pp. 10102-10107, 2011.

[29] W. J. Parker, R. J. Jenkins, C. P. Butler and G. L. Abbott, "Flash Method of Determining Thermal Diffusivity, Heat Capacity, and Thermal Conductivity," Journal of Applied Physics, vol. 32, pp. 1679-1684, 1961.

[30] D. Xiao, Q. Wang, Z. Wang, Y. Zhang, J. Wu, K. Fan, L. Sun, M. Zhu, Z. K. Ng, E. H. T. Teo and F. Hu, "Real-Time THz Beam Profiling and Monitoring via Flexible Vertically Aligned Carbon Nanotube Arrays," Advanced Optical Materials, vol. 10, no. 21, p. 2201363, 2022.

[31] Z. Yin, H. Wang, M. Jian, Y. Li, K. Xia, M. Zhang, C. Wang, A. Wang, M. Ma, Q.-s. Zheng and Y. Zhang, "Extremely Black Vertically Aligned Carbon Nanotube Arrays for Solar Steam Generation," American Chemical Society, vol. 9, no. 34, pp. 28596-28603, 2017.

[32] S. Neupane, M. Lastres, M. Chiarella, W. Li, Q. Su and G. Du, "Synthesis and field emission properties of vertically aligned carbon nanotube arrays on copper," Carbon, vol. 50, no. 7, pp. 2641-2650, 2012.

[33] M. F. De Volder, S. H. Tawfick, R. H. Baughman and A. J. Hart, "Carbon Nanotubes: Present and Future Commercial Applications," Science, vol. 339, no. 6119, pp. 535-539, 2013.

[34] M. E. Itkis, F. Borondics, A. Yu and R. Haddon, "Bolometric Infrared Photoresponse of Suspended Single-Walled Carbon Nanotube Films," Science, vol. 312, no. 5772, pp. 413-416, 2006.